JOURNAL OF MATERIALS SCIENCE 19 (1984) 501–508

Slow crack growth in cellulose fibre cements

Y. W. MAI, M. I. HAKEEM
Department of Mechanical Engineering, University of Sydney, Sydney, NSW 2006, Australia

Slow stable crack growth is a prominent feature of the fracture behaviour of cellulose fibre cements. It is shown that this characteristic can be described by crack growth resistance against crack extension curves based on linear elastic fracture mechanics. Double-cantilever-beam specimens with side grooves are used to obtain such crack resistance curves for a commercial cellulose cement containing approximately 8% mass fraction of bleached fibres. Both dry and wet samples are tested. Compliances measured during slow crack growth by the unloading/reloading technique at successive crack increments are less than those obtained for saw-cut notches with similar crack lengths. Residual displacements due to either mismatch fracture surfaces or a large inelastic process zone at the crack tip are also observed at zero load. A modified elastic potential energy release rate (G_R^*), and hence its equivalent K_R^* [$= (EG_R^*)^{1/2}$], must be used to include this residual displacement effect in order to yield the true crack growth resistance curves. This is found to be necessary for the wet samples due to their large residual displacements. The crack growth resistances of the wet samples are superior to those of the dry samples: this is explained in terms of the improved ductility and toughness of the wet cellulose fibres.

1. Introduction

In our previous work on cellulose fibre cements [1, 2] we showed that their mechanical properties are sufficient to make them useful for many non-structural applications. In a limited way, therefore, they could be used to replace asbestos fibre cements. Bleached cellulose fibres gave better flexural strength and elastic modulus but poorer fracture resistance than unbleached fibres [2]. It was also shown that water absorption had a dramatic adverse effect in decreasing the elastic modulus and strength properties of the composites. However, water absorption also produced an unexpected large increase in the fracture resistance. This was explained in terms of the increase in ductility of the wet fibres which enhanced the fracture toughness of the composite.

The fracture resistance for the cellulose fibre cements reported in [1, 2] was obtained from three-point notched bend specimens using the work of fracture method which was first introduced by Tattersall and Tappin [3]. Basically, the total fracture work given by the area under the load–displacement (P–δ) curve is divided by the fractured ligament area, giving the specific fracture resistance (R) required. R obtained in this way is the maximum fracture toughness that can be developed in the composite. It does not however consider the phenomenon of slow crack growth which is prominent in the fracture behaviour of these fibre cements. To incorporate this effect an alternative method to characterize the fracture of cementitious composites is to use slow crack growth resistance curves, whether G_R (potential energy release rate) or K_R (stress intensity factor) curves, plotted against the crack extension (Δa) [4–11]. The use of G_R or K_R curves for predicting fracture instabilities due to size or geometric effects in metals is well understood and documented [12], but its application to fibre cements has only recently been demonstrated [5, 8]. Although at present it is not clear whether the crack growth resistance curve for fibre cements is a material property independent of size and geometry, there is increasing experimental evidence that this may be so [4, 7, 9].

0022–2461/84 $03.00 + .12

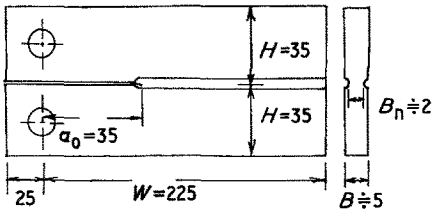

Figure 1 The double-cantilever-beam specimen geometry.

In the present work we have studied slow crack growth in a commercial cellulose fibre cement using the G_R and K_R curve approach. Both dry and wet composites were investigated with double-cantilever-beam specimens. The experimental results were analysed using analytical K-solutions and compliance measurements within the framework of linear elastic fracture mechanics.

2. Experimental work

The cellulose fibre cement composites were supplied by James Hardie & Co. Pty. Ltd in the form of 5 mm thick sheets. They contained 50:50 cement/silica and bleached cellulose fibres (from Western Hemlock pulp) of mass fraction approximately 8%. The densities of the composite sheets varied between 1.28 and 1.31 g cm^{-3}. Three-point flexural tests were conducted on rectangular strip specimens in an Instron testing machine for both the machine and cross directions. The elastic modulus in bending (E) and the flexural strength (σ_b) were calculated from these results. Fracture experiments were performed on double-cantilever-beam (DCB) specimens (Fig. 1) in the Instron testing machine with a very slow cross-head rate of 0.1 mm min^{-1} so as to allow careful observation of slow crack growth during loading. Compliance measurements were taken using the interrupted unloading and reloading technique (see Figs. 3 and 4). It was found out that the grooves on either side of the DCB specimen were needed to maintain a straight crack even though the intended crack propagation was in the weak machine direction. The resultant net section thickness, B_n, was about 2 mm. All the tensile and fracture tests were performed on both wet and dry samples. Wet samples were prepared by immersion in water for 72 h prior to testing and dry samples were oven-dried at a temperature of about 120° C for 24 h.

3. Results and discussion

3.1. Strength and modulus results

Table I gives the flexural strength and elastic modulus results for cellulose cements in both dry and wet conditions. There is a distinct orientation effect on these two mechanical properties, which are higher in the machine direction than in the cross direction. This orientation effect is also observed for other types of cellulose fibre cements [2] and is believed to be a characteristic of the Hatschek process used to produce the sheets. The significant reductions in σ_b and E due to water absorption are also apparent from Table I.

3.2. Fracture results

3.2.1. Fracture mechanics analysis

In order to obtain the crack growth resistance curve we must calculate either K_R or G_R as a function of crack extension (Δa). Based on linear elastic fracture mechanics concepts the stress intensity factor and elastic potential energy release rate may be computed as follows. For the DCB specimen shown in Fig. 1 we have from [13]

$$K_R^2 = \frac{12P^2}{BB_n}\left(\frac{a^2}{H^3}\right)\left[1 + 1.32\left(\frac{H}{a}\right) + 0.532\left(\frac{H}{a}\right)^2\right] \quad (1)$$

where P is the fracture load corresponding to the current crack length a, B and B_n are the specimen gross and net section thicknesses, and H is the beam depth. Equation 1 is valid for the range of crack lengths given by $a/H > 1.5$ and $(W-a)/H > 1.5$ [13, 14]. By measuring (P, a) values at successive intervals of Δa during slow crack growth a curve of K_R against Δa can be constructed.

The potential energy release rate (G_R) is given by

$$G_R = \frac{P^2}{2B_n}\frac{d}{da}\left(\frac{\delta}{P}\right) \quad (2)$$

TABLE I Strength and modulus results for cellulose fibre cements

	Dry samples		Wet samples	
	E (Gpa)	σ_b (MPa)	E (GPa)	σ_b (MPa)
MD	9.65 ± 0.64	22.30 ± 1.70	5.50 ± 0.71	15.8 ± 0.85
CD	8.45 ± 0.78	18.25 ± 2.05	2.95 ± 0.64	11.2 ± 1.27

MD = machine direction; CD = cross direction.

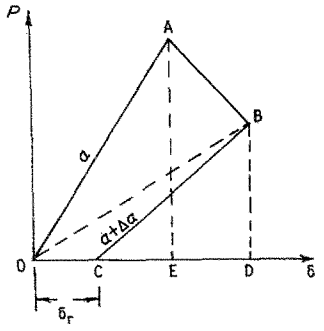

Figure 2 Schematic load (P) against displacement (δ) curves for crack propagation with and without residual displacements (δ_r).

where (δ/P) is the compliance (C) and for the DCB specimen considered this is [13]

$$C = \frac{\delta}{P} = \frac{24}{EB}\left[0.33\left(\frac{a}{H}\right)^3 + 0.66\left(\frac{a}{H}\right)^2 + 0.532\left(\frac{a}{H}\right)\right]. \quad (3)$$

K_R and G_R in linear elastic fracture mechanics are connected by the relation

$$EG_R = K_R^2 \quad (4)$$

and this relation can be proved by substituting Equation 3 into Equation 2 and comparing with Equation 1. Implicit in Equations 1, 2 and 4 is the requirement that the material behaves globally elastically so that, in terms of Fig. 2, unloading after a crack increment Δa should follow BO back to the origin. However, it is observed experimentally both in this work and in others [9, 10, 14] that the unloading path is more likely to follow BC, so that there is a residual displacement $\delta_r(= OC)$ at zero load. It is not clear whether δ_r is caused by plastic bending of the beams, a large process zone size, or collapsed fibres/aggregate interlocked behind the crack tip. From Fig. 2 it is possible to derive an expression for the elastic potential energy release rate absorbed in the fracture process (G_R^*) in the presence of a permanent deformation (δ_r). The strain energy release is the difference between the triangles BCD and AEO. For elastic deformation the strain energy is given by

$$U = \tfrac{1}{2}P\delta = \tfrac{1}{2}P^2\left(\frac{\delta}{P}\right) = \tfrac{1}{2}P^2C^*. \quad (5)$$

C^* is used here to show that it is the compliance measurement when residual displacements are present. It is therefore different from C defined by Equation 3 where $\delta_r = 0$. The strain energy release rate is therefore

$$\frac{dU}{da} = PC^*\frac{dP}{da} + \frac{P^2}{2}\frac{dC^*}{da}. \quad (6)$$

The total external work is given by the area ABDE (Fig. 2). Let us assume that a fraction α of this goes into plastic work and $(1-\alpha)$ goes into essential fracture work. Then we have the modified potential energy release rate given by

$$G_R^* = \frac{(1-\alpha)}{B_n}P\frac{d\delta}{da} - \frac{PC^*dP}{B_n da} - \frac{P^2}{2B_n}\frac{dC^*}{da}. \quad (7)$$

For the fracture of asbestos and cellulose cements it is probable that all the external work goes into useful fracture work so that $\alpha = 0$ [9, 14]. Equation 7 can be rewritten as

$$G_R^* = \frac{P}{B_n}\frac{d\delta}{da} - \frac{PC^*dP}{B_n da} - \frac{P^2}{2B_n}\frac{dC^*}{da}. \quad (8)$$

Now,

$$\delta = \delta_r + PC^*. \quad (9)$$

Differentiating δ in Equation 9 with respect to a and substituting into Equation 8 we have

$$G_R^* = \frac{P^2}{2B_n}\frac{dC^*}{da} + \frac{P}{B_n}\frac{d\delta_r}{da}. \quad (10)$$

When $\delta_r = 0$, $C^* = C$ and $G_R^* = G_R$. When $\delta_r \neq 0$, it can be shown that

$$G_R^* = G_R + \frac{P}{2B_n}\frac{d\delta_r}{da}. \quad (11)$$

The determination of G_R^* using Equation 10 requires that the actual unloading/reloading compliance in the presence of residual displacement (C^*) and δ_r be measured as functions of crack length (a). An equivalent K_R^* can be defined for G_R^* by

$$K_R^{*2} = EG_R^*. \quad (12)$$

Equations 2 and 10 may now be used to construct G_R or G_R^* against Δa curves during slow crack growth. For the G_R-curve the compliances (C) do not include the effect of δ_r but for the G_R^*-curve this residual displacement effect is dealt with as in Equation 10. In addition to the K_R-curve given by the theoretical Equation 1 it is possible to obtain two other K_R-curves based on Equations 4 and 12 using G_R and G_R^* values measured separately. Previous work on asbestos cements [14] has shown that the same slow crack

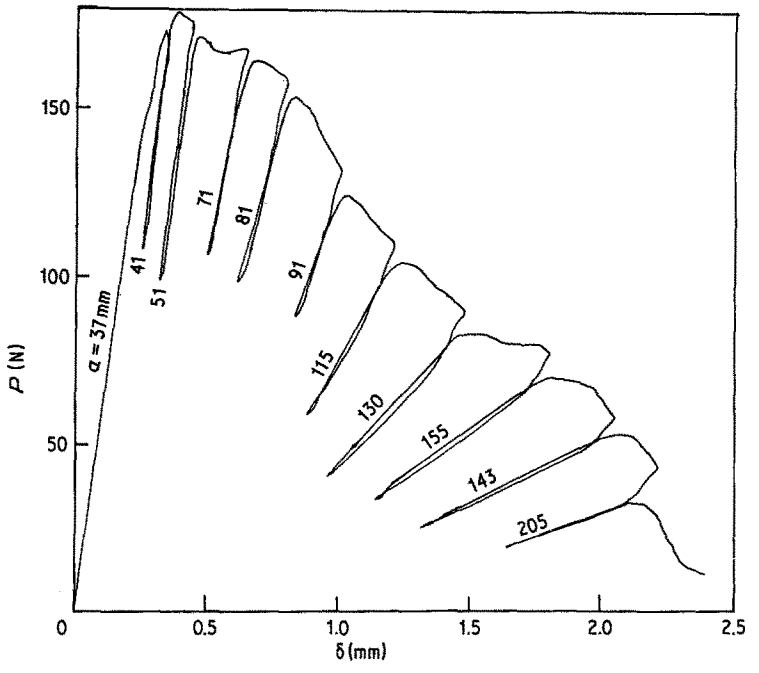

Figure 3 Typical load (P) against displacement (δ) records for crack propagation in dry cellulose fibre cements.

growth resistance curve is obtained whether G_R or G_R^* is used and whether K_R (Equations 1 and 4) or K_R^* is employed. It seems difficult to reconcile these results since it is clearly stated that δ_r is not insignificant [14] whereas the theory requires that $\delta_r \to 0$ in order to obtain identical crack growth resistance curves. In the following section we examine the crack growth resistance curves for dry and wet cellulose fibre cements using these various fracture parameters.

3.2.3. Crack growth resistance curves

Figs. 3 and 4 show typical load–displacement curves during slow crack growth in a dry and a wet sample of the cellulose fibre cement. Against each unloading and reloading line is marked the crack length (a) and the inverse slope of the reloading line gives the compliance C^*. The load at which the reloading curve deviates from linearity is taken as the onset of crack growth and is used to calculate G and K values for the construction of slow crack

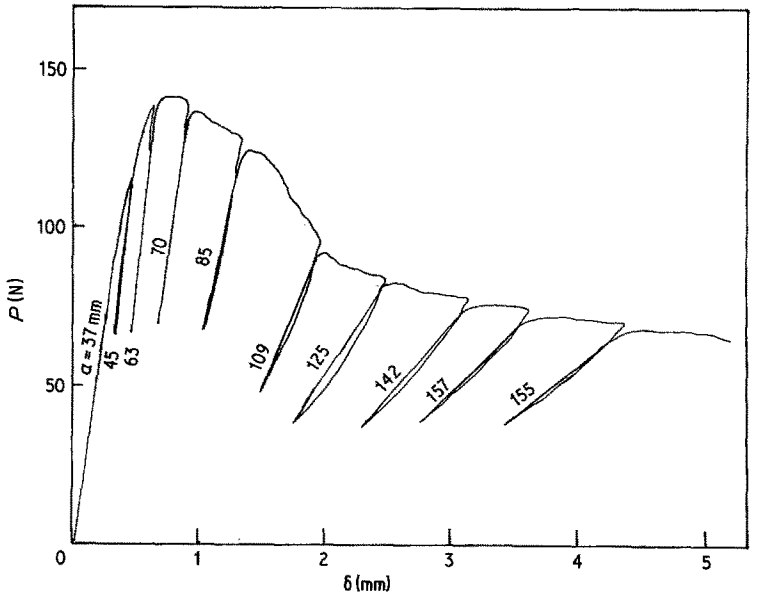

Figure 4 Typical load (P) against displacement (δ) records for crack propagation in wet cellulose fibre cements.

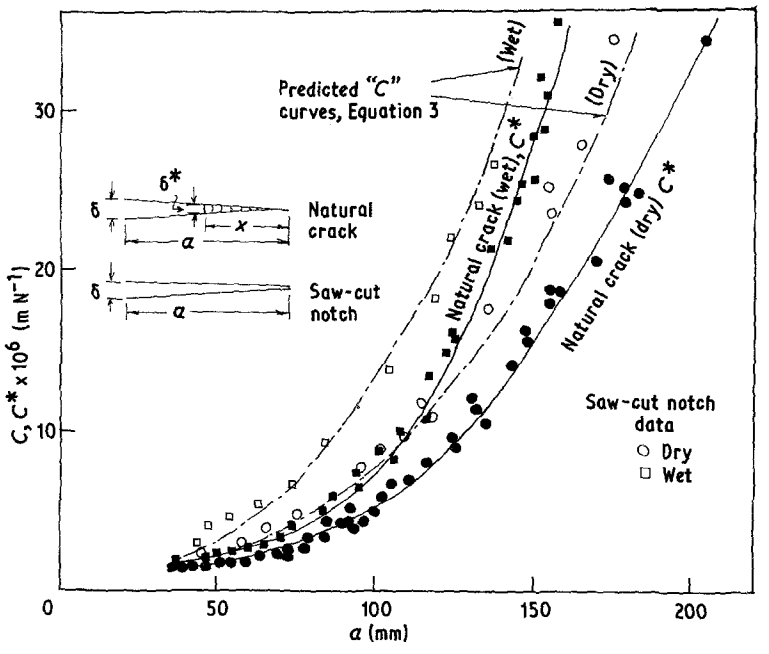

Figure 5 Compliance curves for the double-cantilever-beam cellulose fibre cement specimens with saw cut notches and propagated cracks.

growth resistance curves. The wet and dry crack propagation compliances (C^*) are shown in Fig. 5 and marked "natural crack" to differentiate it from the "saw-cut notch" where there are no bridging fibres left behind the crack tip. For comparison purposes the compliances of samples with "saw-cut" notches of varying crack lengths are also shown in this figure. Quite clearly, for the same physical crack length, the "natural cracks" with bridging fibres tend to decrease the compliances compared with samples where there are no such fibres. As expected, the "saw-cut notch" compliances fit the theoretical predicted C curves given by Equation 3 (with $E_{dry} = 9.70$ GPa and $E_{wet} = 5.5$ GPa) very well for both dry and wet samples.

It is apparent from Figs. 3 and 4 that upon unloading to zero load after crack extension there is a permanent deformation (δ_r). The variation of δ_r with a for dry and wet samples is shown in Fig. 6. For the dry specimens δ_r was very small (approximately 0.75 mm) even at the largest crack length of 200 mm. It is thought that such a small residual displacement may be explained by the mismatch of fracture surfaces due to either bridging fibres or tiny interlock aggregates behind the crack tip. A lesser influence is perhaps due to the process zone ahead of the crack tip in these dry samples. With reference to the inset of Fig. 5, if x is the maximum fibre bridging distance and δ^* is the opening at the wake of this zone, then the residual displacement δ_r at the point of load

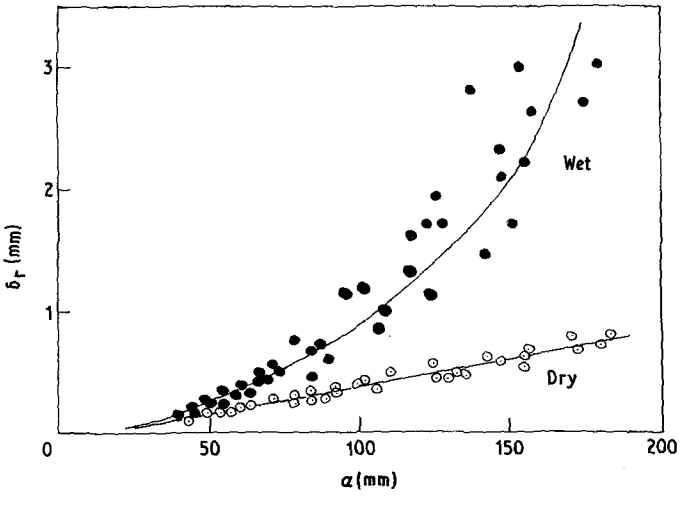

Figure 6 Variation of residual displacement (δ_r) with crack length (a).

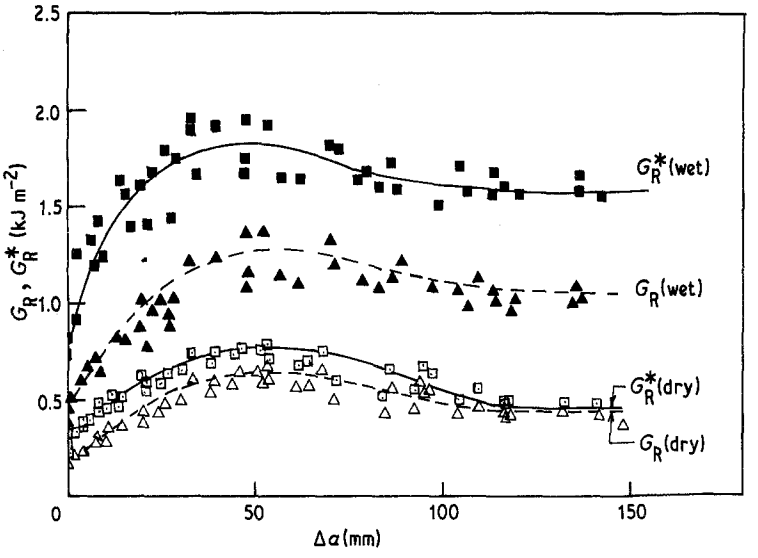

Figure 7 Crack growth resistance (G) plotted against crack extension (Δa) for dry and wet cellulose cements.

application is given by elastic beam deflection theory, so that

$$\delta_r = \frac{\delta^*}{2}\left[\frac{3}{2}\left(\frac{a}{x}\right) - 1\right]. \qquad (13)$$

For $a = 200$ mm, $x \doteqdot 60$ mm, $\delta_r = 0.75$ mm (from Fig. 6), Equation 13 gives $\delta^* \approx 0.16$ mm, which is very small indeed and is of the order of magnitude of the broken fibres protruding from the fracture surfaces.

The variation of δ_r with crack length for the wet samples is non-linear and its magnitude is much larger than for the dry samples at similar crack lengths (see Fig. 6). If Equation 13 is applied here for the same maximum crack length ($a =$ 200 mm) for which $\delta_r \doteqdot 3.5$ mm (Fig. 6) we estimate $\delta^* \doteqdot 0.80$ mm. This very large value can only be explained in terms of the highly deformed fibres and a large process zone size in the wet state.

If in Figs. 3 and 4 we neglect δ_r and draw compliance lines (C) for each crack length (a) by connecting the origin and the corresponding fracture loads (e.g. line OB in Fig. 2) we observe that for the dry samples they agree well with the "saw-cut notch" compliances given in Fig. 5. This means that the dry specimen is still globally elastic and had the fibres been absent unloading would produce zero displacement at zero load. For the wet samples the compliances (C) measured in this way are always larger than the "saw-cut notch" compliances. This strongly suggests that inelastic work at the fracture process zone is large and that the zone size is not insignificant.

Slow crack growth resistance curves for the dry and wet composites are shown in Figs. 7 to 9. The data shown were obtained from four separate experiments for each test condition. In Fig. 7 G_R^* is calculated from Equation 10 and G_R from Equation 11. It is clear that for the dry samples the G_R^* and G_R against Δa results are quite similar, particularly at large crack lengths. For smaller crack lengths less that 80 mm G_R are consistently lower than G_R^* but the maximum difference is no more than 25%. These results are expected since δ_r is small for the dry samples and G_R tends to G_R^* in the limit. However, for the wet samples, δ_r is large and consequently the G_R results which neglect this permanent displacement are only about half of the true G_R^* against Δa results.

From Equations 4 and 12 we can construct equivalent K_R and K_R^* against Δa curves using these G_R and G_R^* against Δa data given in Fig. 7. These curves are shown for the dry samples in Fig. 8 and wet samples in Fig. 9. K_R values predicted from the analytical expression of Equation 1 are also shown in these figures. For the dry samples we must have K_R (from Equation 1) the same as those from K_R $[= (EG_R)^{1/2}]$ since they both assume linear elasticity to be obeyed by the material. Also, as δ_r is small, K_R^* $[= (EG_R^*)^{1/2}]$ should be approximately equal to the other two K_R calculations. These points are borne out by the similar K_R against Δa results given in Fig. 8 even though different equations are used. For the wet samples given in Fig. 9 all these K_R curves are different. The K_R-curve based on the analytical expression, Equation 1, gives the worst results and

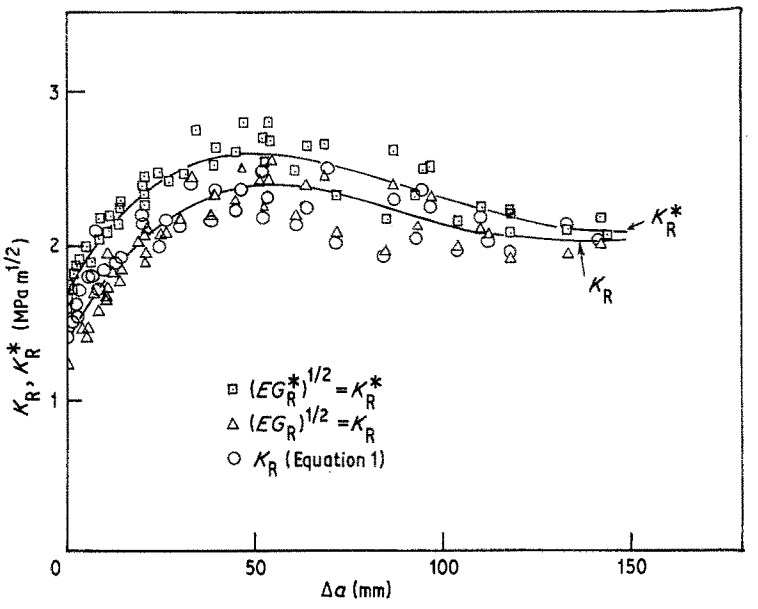

Figure 8 Crack growth resistance (K) plotted against crack extension (Δa) for dry samples.

the one based on G_R without considering residual displacements, i.e. $K_R = (EG_R)^{1/2}$, still underestimates the true K_R^* results given by the uppermost curve.

It is of interest to point out here that the G_R- and K_R-curves both rise slowly with crack growth to a maximum value at some 50 to 60 mm crack growth and then drop gradually to a constant value for crack increments larger than about 100 mm. The drop after the maximum point was not observed in asbestos cements in our previous work [4, 7], although it has been recorded for another asbestos cement in [14]. It is expected that in normal circumstances once the maximum K_R or G_R value is reached steady-state crack propagation corresponding to the translation of the whole fibre bridging zone is established and that this maximum value is maintained with further crack extension. We cannot therefore offer any theoretical reasons for the present cellulose fibre cement results.

In order to explain the much larger crack

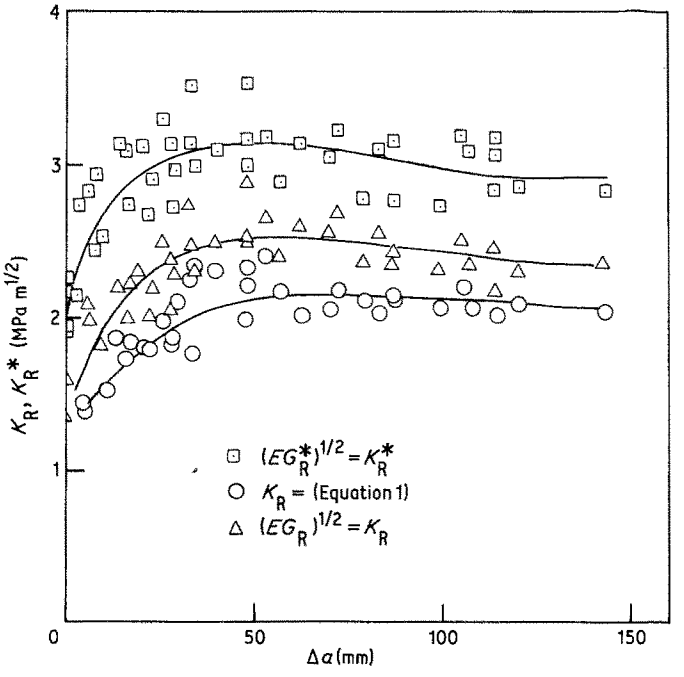

Figure 9 Crack growth resistance (K) plotted against crack extension (Δa) for wet samples.

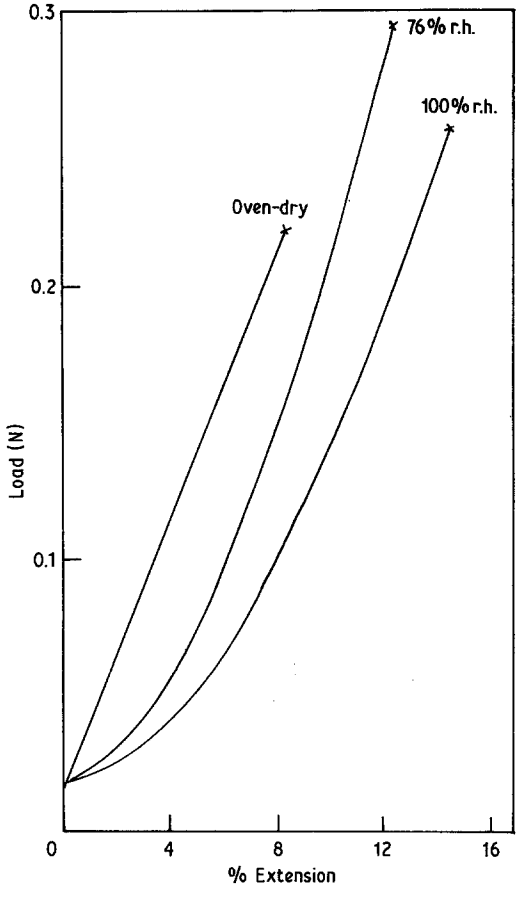

Figure 10 Tensile test results on single cellulose fibres.

growth resistance of the wet samples it is suggested in [2] that this is caused by the large irreversible work absorbed in stretching and unravelling the wet cellulose fibres as well as the subsequent work done pulling out these fibres from their matrices. Some initial work has been done on the fibres by conducting micro-tensile tests on single filaments using the facilities of the James Hardie Research Laboratory. Typical load–extension records for dry and wet fibres are given in Fig. 10 and they confirm the high ductility and larger energy absorption of the wet fibres.

4. Conclusions

Slow crack growth in cellulose fibre cements was investigated in terms of the crack growth resistance curves using either G_R (G_R^*) or K_R (K_R^*) as the characterizing fracture parameter. It is concluded that linear elastic fracture mechanics concepts can be used for these fibre cements. For the dry composites neglecting the residual displacement does not significantly affect the K_R and G_R-curves. However, for wet composites the residual displacements are large and must be included in calculating the true K_R^* and G_R^*-curves. It is also shown that the crack growth resistance curve is much higher for wet than dry composites due to the different deformation behaviour of the fibre in these two states.

Acknowledgements

We wish to thank James Hardie & Co. Pty. Ltd. for financially supporting this research work. Special thanks are due to B. Cotterell for stimulating discussions over several aspects of the fracture analysis given in this paper.

References

1. R. ANDONIAN, Y. W. MAI and B. COTTERELL, *Int. J. Cement Composites* **1** (1979) 151.
2. Y. W. MAI, M. I. HAKEEM and B. COTTERELL, *J. Mater. Sci.* **18** (1983) 2156.
3. H. G. TATTERSALL and G. TAPPIN, *ibid.* **1** (1966) 296.
4. Y. W. MAI, R. M. L. FOOTE and B. COTTERELL, *Int. J. Cement Composites* **2** (1980) 23.
5. J. C. LENAIN and A. R. BUNSELL, *J. Mater. Sci.* **14** (1979) 321.
6. Y. W. MAI, *ibid.* **14** (1979) 2091.
7. R. M. L. FOOTE, B. COTTERELL and Y. W. MAI, in "Advances in Cement–Matrix Composites", Proceedings, Symposium L, Materials Research Society Annual Meeting, Boston, MA, USA 17–18 November, 1980, pp. 95–106.
8. Y. W. MAI and B. COTTERELL, *Int. J. Cement Composites* **4** (1982) 33.
9. M. WECHARATANA and S. P. SHAH, *Proc. ASCE, J. Structural Division* **108** (1982) 1400.
10. K. VISALVANICH and A. E. NAAMAN, ASTM STP 745, 1981, pp. 141–156.
11. C. SOK and J. BARON, Cement and Concrete Research, 9 (1979) 641.
12. "Fracture toughness evolution by *R*-curve methods", ASTM STP 527 (American Society for Testing and Materials, Philadelphia, 1973).
13. S. M. WIEDERHORN, A. M. SHORB and R. L. MOSS, *J. Appl. Phys.* **39** (1968) 1562.
14. K. VISALVANICH and A. E. NAAMAN, *Proc. ASCE, J. Engineering Mechanics Division* **107** (1981) 1155.

Received 23 May
and accepted 26 May 1983